Article

Polyurethane Organosilicate Nanocomposites as Blood Compatible Coatings

Johnson H. Y. Chung [1], Menno L. W. Knetsch [2], Leo H. Koole [2], Anne Simmons [1] and Laura A. Poole-Warren [1,*]

[1] Graduate School of Biomedical Engineering, University of New South Wales, NSW 2052, Australia; E-Mails: j.chung@student.unsw.edu.au (J.H.Y.C.); a.simmons@unsw.edu.au (A.S.)

[2] Department of Biomedical Engineering/Biomaterials Science, University of Maastricht, P.O. Box 616, 6200 MD Maastricht, The Netherlands; E-Mails: menno.knetsch@maastrichtuniversity.nl (M.L.W.K.); l.koole@maastrichtuniversity.nl (L.H.K.)

* Author to whom correspondence should be addressed; E-Mail: l.poolewarren@unsw.edu.au; Tel.: + 61-2-9385-7662; Fax: +61-2-9385-5949.

Abstract: Polymer clay nanocomposites (NCs) show remarkable potential in the field of drug delivery due to their enhanced barrier properties. It is hypothesised that well dispersed clay particles within the polymer matrix create a tortuous pathway for diffusing therapeutic molecules, thereby resulting in more sustained release of the drug. As coatings for medical devices, these materials can simultaneously modulate drug release and improve the mechanical performance of an existing polymer system without introducing additional materials with new chemistries that can lead to regulatory concerns. In this study, polyurethane organosilicate nanocomposites (PUNCs) coated onto stainless steel wires were evaluated for their feasibility as blood compatible coatings and as drug delivery systems. Heparin was selected as the model drug to examine the impact of silicate loading and modifier chain length in modulating release. Findings revealed that better dispersion was achieved from samples with lower clay loadings and longer alkyl chains. The blood compatibility of PUNCs as assessed by thrombin generation assays showed that the addition of silicate particles did not significantly decrease the thrombin generation lag time (TGT, $p = 0.659$) or the peak thrombin ($p = 0.999$) of polyurethane (PU). PUNC coatings fabricated in this research were not cytotoxic as examined by the cell growth inhibition

assay and were uniformly intact, but had slightly higher growth inhibition compared to PU possibly due to the presence of organic modifiers (OM). The addition of heparin into PUNCs prolonged the TGT, indicating that heparin was still active after the coating process. Cumulative heparin release profiles showed that the majority of heparin released was from loosely attached residues on the surface of coils. The addition of heparin further prolonged the TGT as compared to coatings without added heparin, but a slight decrease in heparin activity was observed in the NCs. This was thought to be from competitive interactions between clay-heparin that influenced the formation of the ternary complex between heparin, ATIII thrombin. In summary, the feasibility of using PUNC as drug delivery coatings was shown by the good uniformity in the coating, absence of by-products from the coating process, and the release of active molecules without significantly interfering with their activity.

Keywords: Polyurethane; nanocomposite; coatings; heparin; drug delivery

---

1. Introduction

Oral or intravenous administration of aggressive anticoagulants and anti-thrombotics is a typical approach to prevent device failure in blood related applications and to improve surgical outcomes. In the case of coronary stents, warfarin, aspirin and clopidogrel are commonly used peri-operatively and for at least 1 year post-operatively [1]. Using anti-thrombotics for long periods of time may introduce bleeding and surgical complications as well as longer hospital stays and higher costs [2]. Some of the strategies used to improve blood compatibility of polymers and reduce requirements for systemic administration of drug therapy are the surface modification of polymers through covalent or non-covalent immobilisation with either anti-thrombotic agents, introduce hydrophilic polymer chains, or incorporation and release of anti-thrombotic agents directly from the bulk material [3,4]. Heparin, a potent anticoagulant drug, interacts strongly with antithrombin III (ATIII) in preventing the formation of a fibrin clot and is commonly chosen as a preferred agent in the aforementioned device modifications.

Extensive research has been conducted on the development and evaluation of immobilised heparin on polymer surfaces. This has been achieved through a variety of techniques including covalent linking via a spacer [5–8], layer-by-layer deposition [9–11], photochemical coupling [12], physical adsorption [13], or in the form of block copolymers [14,15]. Conversely, it has been reported that heparin can be released from polymers through both ion-exchange mechanisms and via diffusion [16]. Control of drug release from polymers can be achieved by a number of approaches, such as modifying the composition or morphology of the polymer to decrease the mobility of the drug or the pore size of the polymer [17], adding an additional layer or coating to increase the diffusion pathway [18,19], or modulating drug distribution to overcome the diminishing release rate [20]. These approaches however, involve extra processing steps and introduction of additional materials that may increase both the cost and time.

In theory, by adjusting the filler content and the dispersion of nanofillers, nanocomposites (NCs) could control drug release without the need for chemical modification, additional coatings or extra processing steps. This is based on the tortuous pathway model where drugs are released through diffusion but are forced to follow a longer path due to the presence of impermeable nanoparticles. Interestingly, reports in literature on polymer NCs for blood applications have focused more on the development of a blood compatible surface rather than achieving compatibility through controlled release of anti-thrombotic molecules [21–23]. In addition, among the NCs reported for blood applications, carbon nanotubes were often selected as the nanofiller rather than clay [21,23,24], and there have been no reports in using polyurethane organosilicate nanocomposites (PUNCs) for blood contacting devices. In the majority of studies cited, materials were also fabricated as films rather than as coatings, and are typically not focused on anti-thrombotic applications [25,26].

Coating polymer clay NCs on metallic surfaces could be extremely useful for devices that have good physical properties but poor blood compatibility. In particular, using polyurethane as the matrix could provide the coating with elasticity, strength, and good baseline blood compatibility [27]. Therefore, the aims of this study were to assess the comparative blood compatibility of PU and PUNCs coatings, and explore the potential of using a NC system as a drug delivery system by examining the impact of silicate loading and modifier chain length in modulating heparin release.

2. Results and Discussion
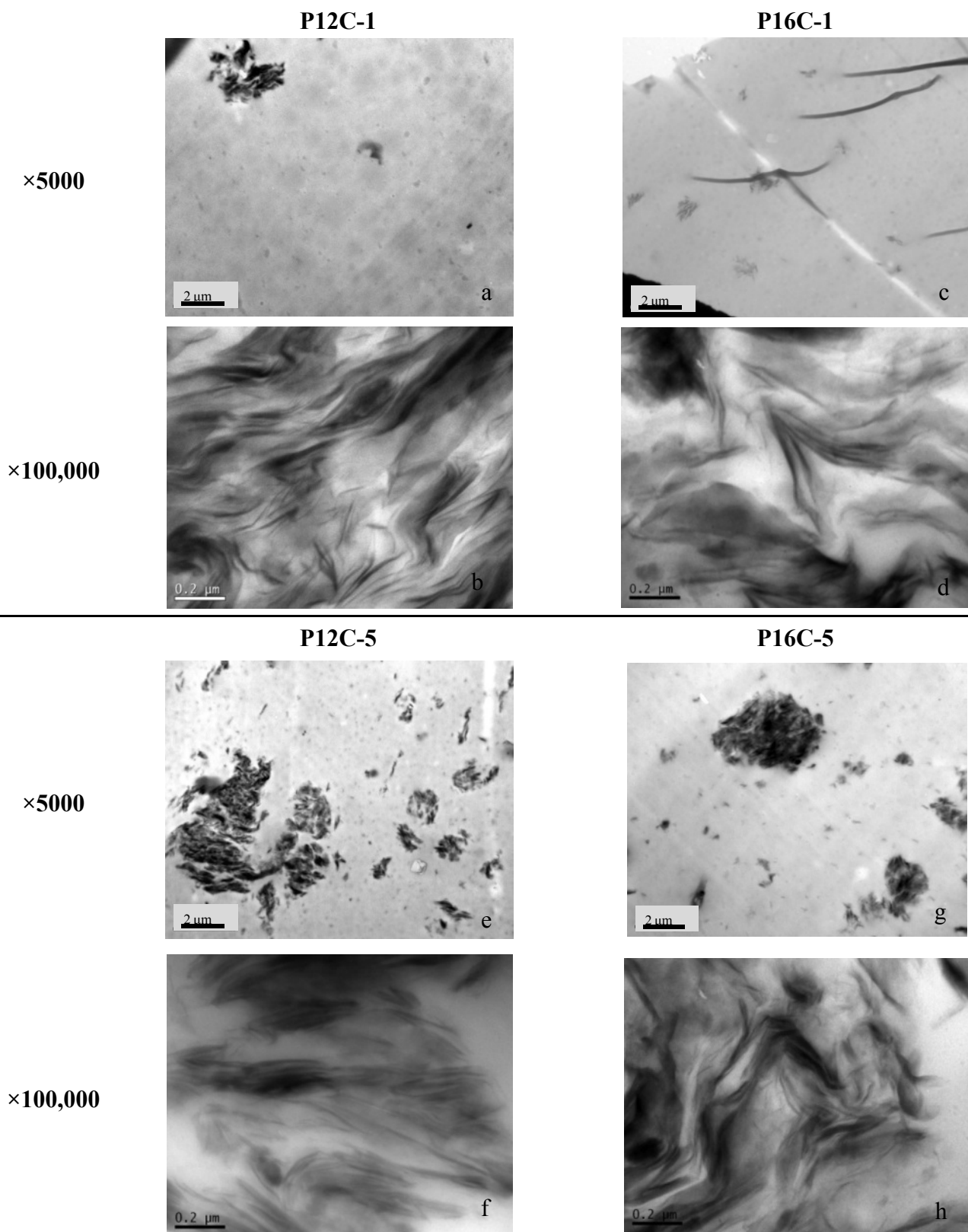
2.1. Silicate Dispersion

Transmission electron microscopy (TEM) and X-ray Diffraction (XRD) were used to study the NC morphologies achieved in the materials. The spacings determined by XRD for PUNCs at varying clay concentrations and different modifier lengths are shown in Table 1. In general, it can be seen that samples with higher clay loadings show more clay aggregation than samples with lower clay loadings. An increase in spacing was also observed with the use of longer alkyl chain modifiers which is in agreement with findings in the literature [28]. There was an absence of peaks for 1 wt % loading in both modifier types implying a partially exfoliated or fully exfoliated morphology.

Table 1. X-ray Diffraction (XRD) results for materials investigated in this study.

Material	2θ	Silicate spacing (nm)
PU	-	-
P12C-1	-	-
P12C-5	3.47	2.55
P16C-1	-	-
P16C-5	2.71	3.26

Representative TEM images of both 1 and 5 wt % loading for P12 and P16 taken is displayed in Figure 1. The increase in clay content resulted in an increased tendency to form clumps and the use of longer chain OM tended to result in smaller clumps, especially between P12C-1 and P16C-1. This was consistent with the XRD findings where increased clay loading decreases the silicate spacing and the use of longer chain length OM resulted in better dispersion.

Figure 1. Representative TEM images of polyurethane organosilicate nanocomposites taken at magnifications of 5000× (scale bar = 2 μm) and 100,000× (scale bar = 0.2 μm) for 1 wt % NCs (**a–d**) and 5 wt % NCs (**e-h**).

At higher magnifications, both P12 and P16 at 1 wt % loadings showed distinguishable individual silicate layers, but still contained regions where clay was not fully exfoliated. However, the XRD analysis for both of these NCs did not display a peak for an intercalated morphology. Therefore, by combining the results of both TEM and XRD, the structure for NCs modified with 1 wt % loadings were classified as partially exfoliated and the absence of peaks from XRD could be due to the distance between silicate layers exceeding the detection limit of this particular X-ray diffractometer. Future studies could involve the use of small angle x-ray scattering (SAXS) to identify the peaks in the 1 wt % loaded samples. Moving onto the 5 wt % loadings, the increase in number of dark regions confirmed the higher tendency of those samples to form clay aggregates and a well ordered multilayer morphology (intercalated) was apparent.

Based on XRD results, the use of longer chain modifiers appeared to improve dispersion within a PUNC system. However, the difference between P12C-1 and P16C-1 shown in Figure 1 did not indicate a substantial difference in clay separation. Given that TEM focuses on a small section at very high magnification, the images obtained may not represent the general dispersion in the bulk of the sample. As indicated previously, although longer chains disperse better, the structure at high clay loadings are still intercalated from both XRD and TEM analysis.

2.2. SEM

Representative SEM images of PUNC coated coils are shown in Figure 2. Under SEM, the coated coils with and without heparin showed similar features and therefore only the coils without heparin were displayed. Notably, wires coated with PU showed a smoother surface with minor debris, while NCs showed a rougher surface which could be due to impurities during silicate preparation and modification. The surface features between 1 wt % and 5 wt % loading were quite similar and the differences between P12s and P16s were not obvious.

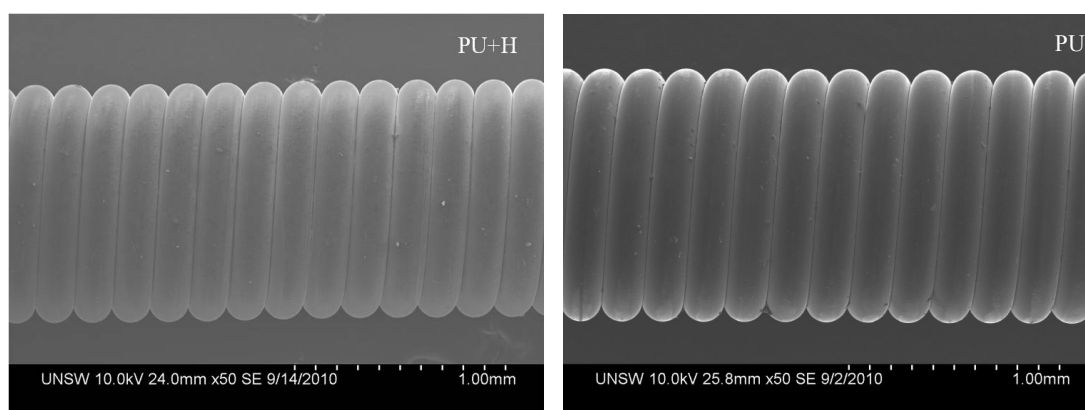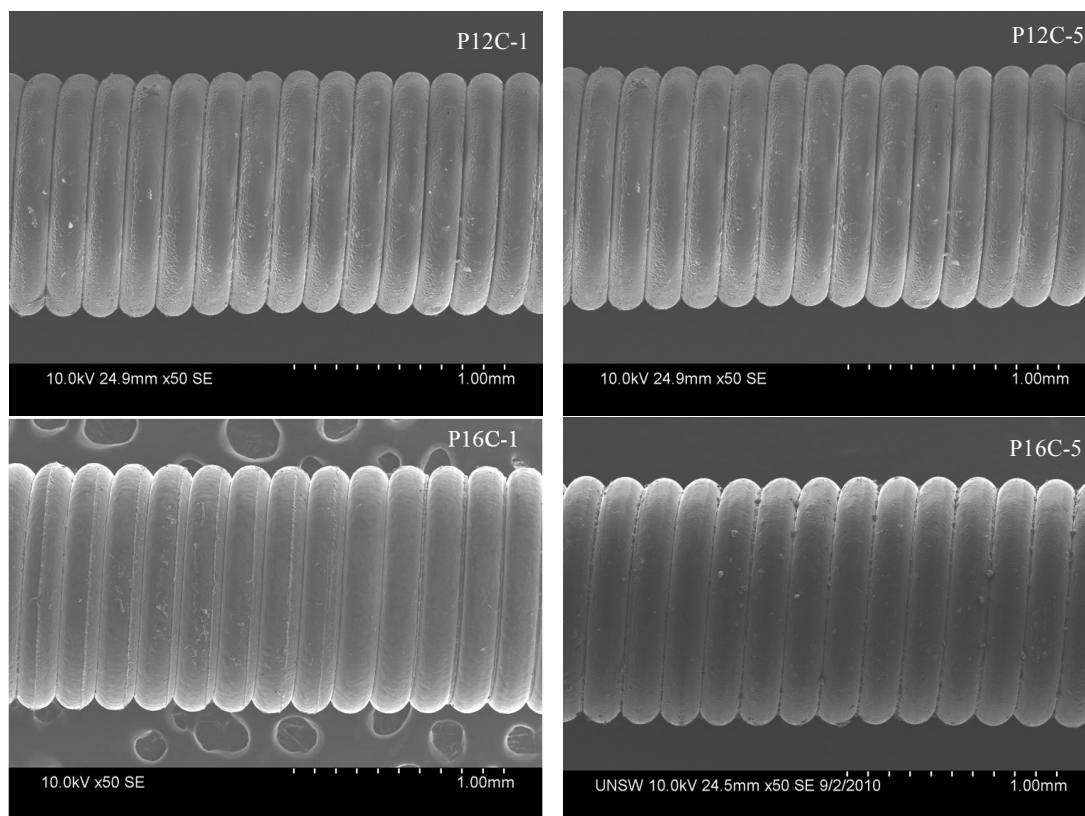**Figure 2**. Representative SEM images of coated coils taken at 50× (scale bar is 1 mm).
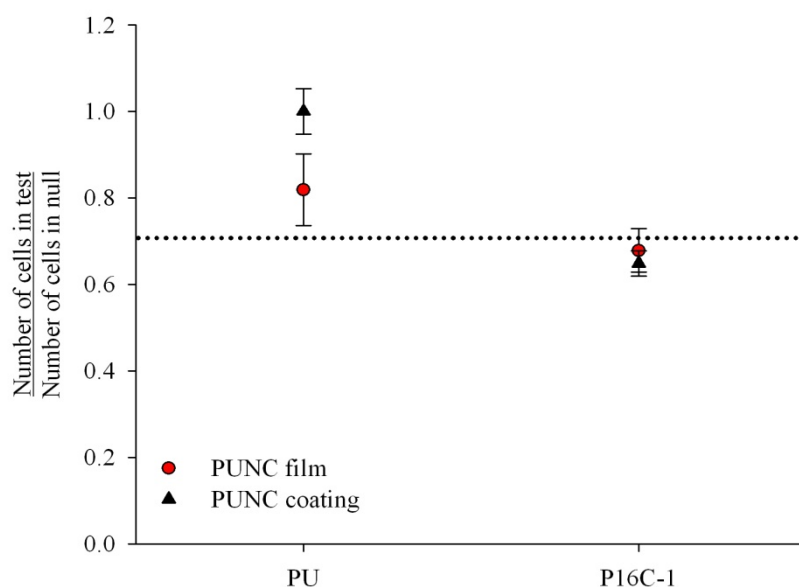
Figure 2. *Cont.*
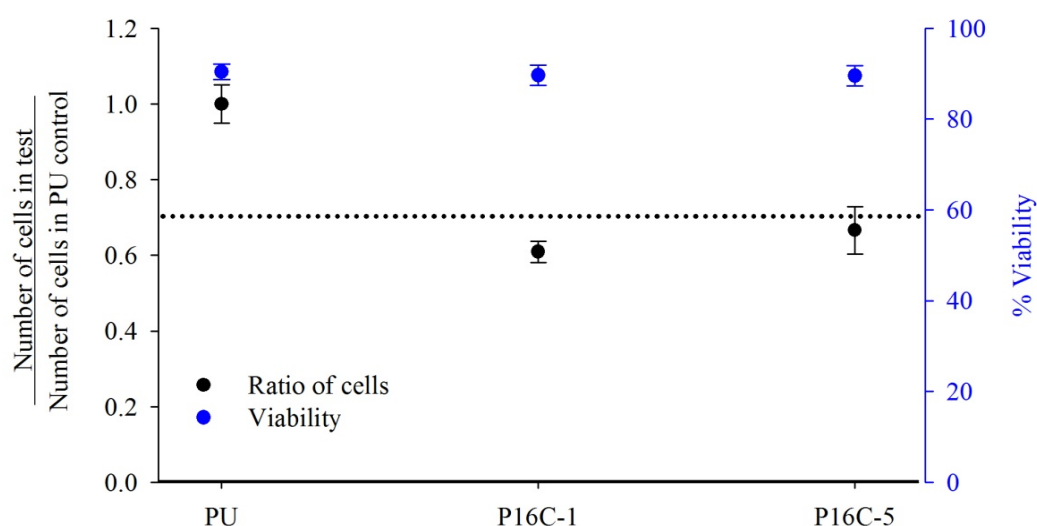

2.3. Cell Growth Inhibition (CGI)

The biological response between PUNCs and mammalian cell lines was investigated using a cell growth inhibition assay. An arbitrary value of 0.7 was used as an indicator in this assay for assessing the "acceptable level" of cell inhibition [29,30]. A comparison between PU and PUNCs fabricated either as films or coatings is shown in Figure 3. PUNCs at 1 wt % clay loading in both cases produced similar levels of inhibition and were not significantly different ($p = 0.535$). On the other hand, the level of inhibition appeared to be lower for PU fabricated as coatings, but were not significantly different ($p = 0.130$) to the films. The similarity in CGI ratio from both fabrication methods suggested that PU and PUNCs can be processed by the automated coating system at MCTec BV (Venlo, The Netherlands) without introducing by-products or contaminants that can affect the cell viability.

The CGI assay of coated coils as compared to pristine PU is shown in Figure 4. Both PUNCs modified with 16CH$_3$ at 1 wt % and 5 wt % clay loading showed CGI bordering the 'acceptable limit' of 0.7, but still maintained a high viability of approximately 90%. One of the reasons for cell growth inhibition may be the presence of OM in the material extracts. It has been reported in the literature that OM during PUNC fabrication could leach out from the material, thus disrupting the cell growth and membrane integrity [31]. Since OMs were not bound to silicate surfaces by covalent bonding but rather through electrostatic interactions, it is possible that these small molecular weight OM can still migrate out of the NC system and impact on the cell growth [31,32].

Figure 3. Comparison of cell growth inhibition of PU and P16C-1 fabricated as films or coatings. Data represents a ratio of the number of cells in the test samples against the number of cells in the null control (cells in media only). Dotted line defines the threshold considered to be an acceptable cell growth inhibition (CGI) level. Mean ± SD (n = 3).

Figure 4. Comparison of cell growth inhibition of PU and PUNCs. Data represents a ratio of the number of cells in the test samples against the number of cells in PU control. Dotted line defines the threshold considered to be an acceptable CGI level. Mean ± SD (n = 3).

The borderline CGI ratio of these samples however, does not necessarily rule out its use within a biological environment. A CGI ratio of 0.7 used in this assay was simply an indicator for assessing the cellular growth. Studies have shown that materials exhibiting adverse *in vitro* behaviour may still show appropriate results *in vivo* [33,34]. The differences between *in vitro* and *in vivo* studies may be due to

higher localised concentrations of cytotoxic or leachable products *in vitro versus* a more diluted case in an implant [33].

2.4. In vitro *Heparin Release*

Figure 5 shows the cumulative release profile of heparin from PUNC coils. All samples demonstrated a rapid initial burst followed by an early plateau. The total heparin released after 24 or 48 h is summarized in Table 2, of which PU + H released the most (25% of total heparin) while P16C-1 + H released the least (16% of total heparin) after 48 h. There was minor difference in the amount of heparin released across all samples between 24 and 48 h as indicated by the plateau in the release profile. A slight increase in heparin was observed from P16C-1 + H in Figure 5 after 24 h. However, when expressed in terms of percentage released, the increase was only 1–2% over 24 h. This showed that the majority of heparin was released from the coils within the first 24 h.

Although a general trend in the release profile was seen to be related to the clay loading and OM chain length, the differences in total heparin released were small. Along with a large burst effect, results suggested that the majority of heparin released from the samples may be from loosely attached heparin residues on the surface after processing. In addition, the retardation in heparin release with increasing clay content was more related to heparin being trapped within the bulk polymer by interactions with clay rather than through diffusion.

Interactions between clay-heparin could actually retard the release if heparin was to follow the tortuous pathway model and diffuse out of the polymer. The fact that the release of heparin reached a plateau in the early stages, suggested that the trapping of heparin within the bulk polymer could also be related to the size of heparin. The conventional heparin used in this study was unfractionated with a mean heparin molecular weight of 15,000 Dalton [35]. Future studies involving heparin release could use low molecular-weight-heparin (LMWH) with an average molecular weight (MW) of 4500 Dalton or other smaller anti-platelet drugs instead [35].
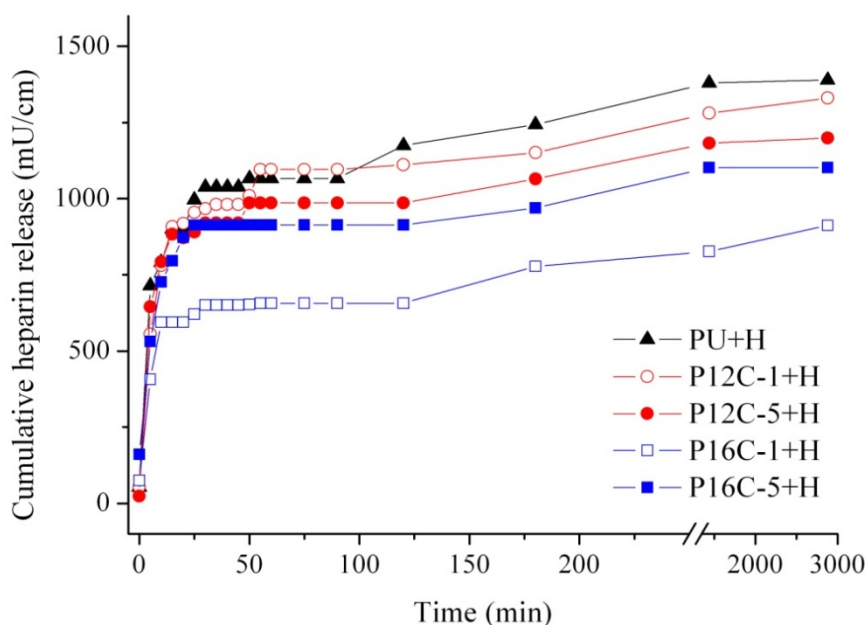
Table 2. Summary of total heparin released. Mean % ± SD.

Material	Total heparin released (% released ± SD)	
	24 h	48 h
PU + H	25 ± 2	25 ± 2
P12C-1 + H	23 ± 1	24 ± 4
P12C-5 + H	21 ± 2	21 ± 5
P16C-1 + H	15 *	16 ± 2
P16C-5 + H	20	20 ± 2

* Indicates significant difference compared to PU control ($p = 0.0586$).

Figure 5. Cumulative release of samples incorporated with heparin for 48 h (n = 2). The error bars in this figure was neglected for ease of interpretation. There was no significant difference in heparin released between 24 to 48 h across all samples. Lines connecting each time point were included for a better representation of the trend of the samples.

2.5. Blood Compatibility

PUNC coated coils were examined for their thrombogenicity as compared to neat PU. Since the continuous release of heparin can interfere with the results obtained from the thrombin generation assay, a pilot study prior to testing was conducted to examine the effect of washing time on heparin activity. The results in Figure 6 suggested that all samples generated similar thrombin generation lag times (TGTs) despite the different washing times (p = 0.131). This not only showed that the heparin bound on the surface was still active after washing, but a washing time of 24 h prior to experimentation was sufficient to remove all loosely attached heparin residues.
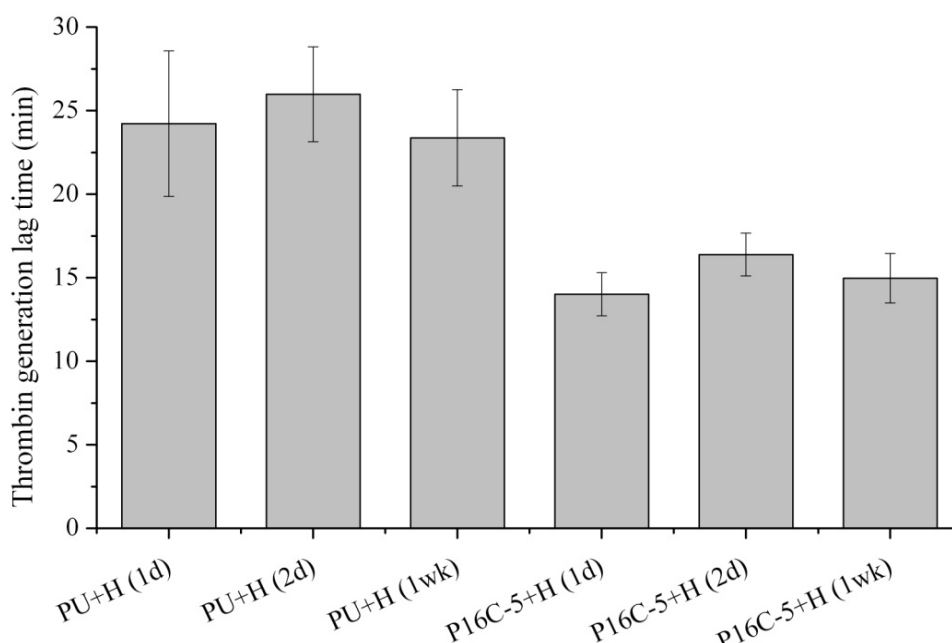
Using coils that were washed for a minimum of 24 h, the average TGT and peak thrombin for the coils is illustrated in Figure 7 and 8 respectively. Interestingly, the addition of silicate particles which increased the surface roughness and debris on the coating as evidenced by SEM, had no effect on the TGTs as compared to neat PU (p = 0.659). This showed that the addition of silicate particles into PU did not increase the thrombogenicity of the material and the blood compatibility of PU was still maintained. The peak thrombin produced by the NCs without heparin was also similar to the amount produced by PU with no significant difference (p = 0.999).

Despite reports suggesting that the covalent binding of PU with linear alkyl chains (16 carbon chain or 18 carbon chain) could reduce the amount of thrombin deposition [36], the results obtained in this study showed no observable trends between clay loading and the use of longer OM chains. The alkylation of PU surfaces was known to increase the initial adsorption of albumin on the surface which reduces platelet and leukocyte adhesion, thereby inhibiting thrombus formation [37,38] It is possible that the binding of clay with OM prevented modifiers rising to the surface of the NC, therefore the
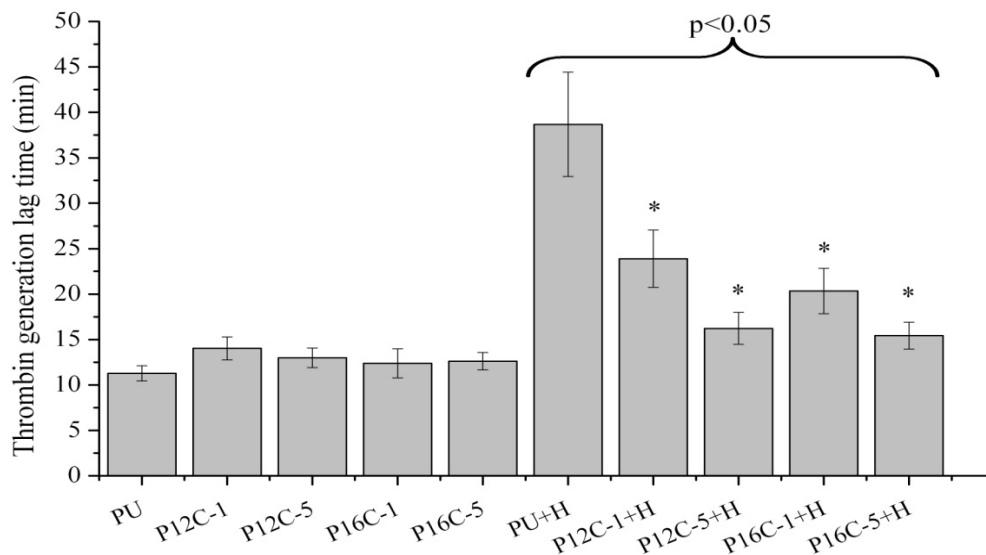
chances for albumin to interact with free alkyl chains were largely limited. Nevertheless, TGT was maintained with the addition of clay, showing that PUNCs can be used in blood related applications.

In relation to biological activity of the released heparin, coils incorporated with heparin displayed significantly longer TGT ($p < 0.05$) and lower peak thrombin ($p < 0.05$) than their relative controls. This showed that the activity of heparin was preserved and was not lost during the coating process. The TGT for PU + H however, was the longest (38.67 min) compared to all heparin loaded samples. It is possible that the presence of clay may have an impact on the electrostatic interactions between the heparin, ATIII and thrombin, which decreases its activity to inhibit thrombus. The interactions between clay-heparin may have neutralised parts of the heparin which in result affected the formation of the ternary complex. In physiological conditions, heparin and ATIII were both reported to be negatively charged and thrombin being positively charged. The accelerated action of heparin results from cooperative electrostatic interaction with thrombin and simultaneous non-ionic with ATIII, where tryptophanyl residues in ATIII were regarded as the non-ionic binding sites for heparin [39]. As OMS consists of positively charged head groups and regions of negative charges from non-exchanged clay surfaces, the interactions between clay-heparin most likely influenced the ability of heparin to bind to both ATIII and thrombin. It has been reported that the hydrolysis of a few N-sulfate residues (negatively charged) on heparin might be sufficient to terminate the action of heparin *in vivo*. The intra-molecular charge neutralisation after hydrolysis may prevent heparin from adapting a stretch out conformation, therefore the interaction sites available with further thrombin is impaired [39].
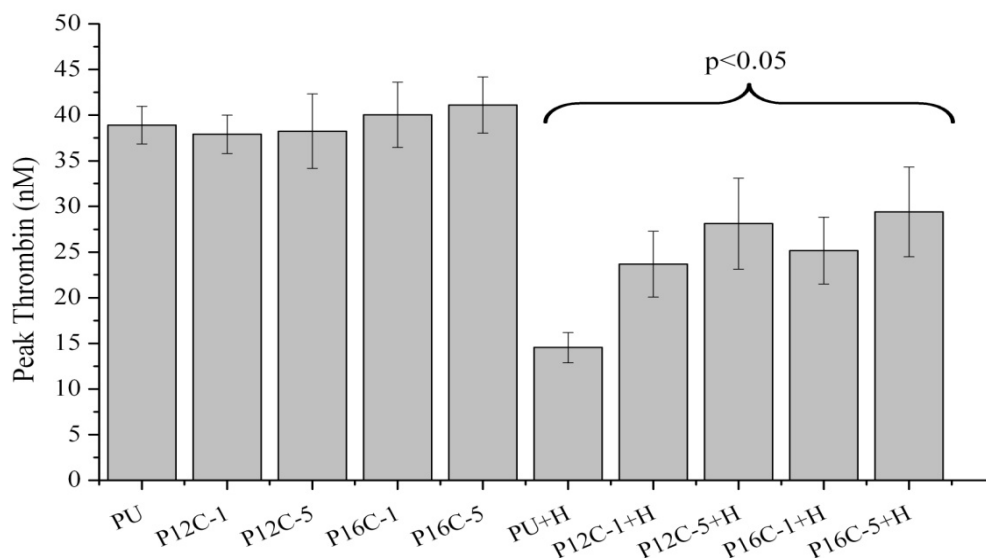
Figure 6. Thrombin generation lag time (TGT) of PU + H and P16C-5 + H under washing times of 1 day, 2 days, and 1 week. Data represents mean ± SD. Statistical analysis indicated no significant difference between the TGT of samples with respect to washing time.

Figure 7. TGT for coils with and without heparin conducted with PRP from 2 donors. Data represents mean ± SD, n = 3. The TGT of heparin incorporated coils were significantly different to coils without heparin ($p < 0.05$). * Denotes heparin incorporated coils significantly different to PU + H.

Figure 8. Peak thrombin of coils with and without heparin conducted with PRP from 2 donors. Data represents mean ± SD, n = 3. The peak thrombin of heparin incorporated coils were significantly different to coils without heparin ($p < 0.05$).

3. Experimental Section

3.1. Materials

Polyurethane (PU) was employed in this study as a model elastomer, consisting of 1000 gmol^{-1} polytetramethylene oxide (PTMO) soft segment and a 4,4'-methylene diphenyl diisocynate (MDI) and 1,4-butanediol (BDO) hard segment. The components were combined in the ratio 100:7.5:46.3 respectively, with 0.003 dibutyltin dilaurate (DBTDL) added as catalyst. The PU was supplied by Urethane Compounds (Melbourne, Australia). Unmodified clay Cloisite Na$^+$ natural montmorillonite (MMT) with CEC of 92.6 meq/100g clay was obtained from Southern Clay Products. Organic modifiers (OM), dodecylamine (12CH$_3$) and hexadecylamine (16CH$_3$) were obtained from Sigma-Aldrich Pty Ltd. NMP (1-methyl-2-pyrrolidone) from Acros, USA was used as the solvent. Unfractionated heparin (Celsus Laboratories Inc, Cincinnati, OH, USA) was used as received. Heparin was present as the sodium salt and the activity was 197 units/mg.

3.2. Modification of Silicates

Organically modified silicates (OMS) were produced by cationically exchanging montmorillonite with organic modifiers. A 5 wt % solution of NaMMT was prepared in Milli-Q water and left stirring at 50 °C for a period of 24 h. Compounds for organic modification were added at 110% of the theoretical CEC of MMT and solutions were then stirred vigorously for 24 h at a temperature of 50 °C. The OMS was then isolated, dried and passed through a 325-mesh (45 μm) sieve.

3.3. Nanocomposite Preparation and Coating

Required amounts of PU and NMP were weighed to achieve 8% w/v PU in NMP suspension and stirred for a period of 5 days to ensure that the PU was completely dissolved. PUNC solutions for coating were prepared by mixing polymer suspension and modified clay overnight. For PUNCs incorporated with heparin, 10 wt % heparin (g heparin/100g PU) dissolved in formamide (Sigma, Aldrich, MO, USA) was added to the NC solution. Two types of modifiers were used to prepare NCs: dodecylamine and hexadecylamine with prefix labeled as P12 and P16 respectively. A suffix was added according to the %OMS and to samples with added heparin (e.g., a NC that contained the OMS 12CH$_3$MMT at 1% OMS loading + heparin would be identified as P12C-1 + H). PUNCs were labelled accordingly as shown in Table 3.

PU and PUNC were coated on stainless steel wires through an automated coating system at MCTec BV (Venlo, The Netherlands). Stainless steel wires (>1000 m, diameter 171 μm) were pulled through the polymer solution at 1.1 m/s and guided through a cylindrical oven (maximum temperature 300 °C) to evaporate the solvent (NMP). Thickness of the coating was monitored with an in-line continuous measurement. Wires used in this study were first coated with 1μm layer of polyether sulphone (PES) as a binder. Following that, a second layer consisting of PUNCs (3 μm) with or without heparin was coated by the same process.

The resulting diameter of the coated stainless steel wires was 176 μm. Coated wires were then coiled by a speed controllable mandrel and a stainless steel core wire with a diameter of 690 μm was

used. Coils of approximately 50 cm in length were made. These coils were used to conduct experiments as they allow more surface area with lesser materials. PU and PUNC films were prepared by solvent casting. Required amounts of OMS and PU suspension were stirred at 60 °C for 17 h to allow polymers to penetrate the clay interlayer. The mixture was then poured into a glass mould (220 mm × 70 mm) and the solvent was removed at 60 °C and 400 mbar in a vacuum oven (Binder V23) for 48 h. Cast films were stored away from light for 7 days prior to characterisation to allow residual solvent to evaporate.

Table 3. Materials investigated within this study.

Material ID	Tested [a]	OMS	Loadings (g/100g PU)	
			Clay	Heparin
PU	F,C	-	-	-
P12C-1	F,C	12CH$_3$MMT	1	-
P12C-5	F,C	12CH$_3$MMT	5	-
P16C-1	F,C	16CH$_3$MMT	1	-
P16C-5	F,C	16CH$_3$MMT	5	-
PU + H	C	-	-	10
P12C-1 + H	C	12CH$_3$MMT	1	10
P12C-5 + H	C	12CH$_3$MMT	5	10
P16C-1 + H	C	16CH$_3$MMT	1	10
P16C-5 + H	C	16CH$_3$MMT	5	10

[a] Samples fabricated as: F = films; C = coatings.

3.4. X-ray Diffraction

XRD is a common technique used to evaluate the spacing between clay layers. The distance between the silicate layers (d spacing) was calculated using Bragg's law (Equation 1), where λ is the wavelength of the incident beam, 2θ is the diffraction angle and *d* is the distance between silicate layers. As more polymer penetrates the interlayer, the d-spacing increases and so the diffraction angle (θ) decreases. Exfoliation occurs when the spacing is sufficiently large that the reflection peaks disappears.

$$\lambda = 2d\sin\theta \qquad (1)$$

Samples of ~15 mm × 60 mm were cut into strips selected randomly from the cast sheets. The distance between silicate layers in the NC was determined on a Philips PW-1830 X-ray diffractometer with CuKα radiation of 0.15406 nm at 40 kV and 40 mA. Strips were scanned from 1.8 to 9° at a rate of 0.00133°/s and a step size of 0.01°. A 1/12° divergence slit and 1/12° anti-scattering slit was used and the data were collected using X'pert Data Collector software.

3.5. Transmission Electron Microscope (TEM)

A small section of the cast NC films was cryosectioned using a Leica FC6 Cryo-Ultramicrotome at a temperature of −120 °C. Slices were cut at a rate of 0.15–3 mm/s to approximately 90–110 nm in thickness and collected onto a 200-mesh copper grid for analysis. Images of the samples were taken

using a JEOL 1400 TEM, with an accelerating voltage of 100 kV. Each sample was imaged at multiple locations and one representative image of the material was chosen for presentation.

3.6. Scanning Electron Microscope (SEM)

The integrity of the coated coils was evaluated using a Hitachi S3400-X SEM. Coils were cut into 2 cm sections and fixed onto a specimen holder by carbon tape. An accelerating voltage of 10 kV and current of 30 mA were used. Each coil was imaged at multiple locations and one representative image of the material was chosen for presentation.

3.7. Cell Growth Inhibition (CGI) Assay

The model cell lines used to conduct biological assays in this study were L929 mouse fibroblast cultured in Eagle's minimal essential medium (EMEM, Sigma Aldrich) supplemented with 10% foetal bovine serum and 1% penicillin/streptomycin (P/S). Cells were seeded at a density of 5×10^4 cells/mL (2 mL) into tissue culture dishes (35 mm) and incubated (37 °C, 5% CO_2) for 24 h. Coils (4 cm sections) or films (punch-cut into 1.5" diameter disc) were sterilised via ethylene oxide (EtO) gas (Prince of Wales Hospital, NSW, Australia) and extracted in EMEM media (4 mL) to give 0.1–0.2 g/mL of extraction vehicle as suggested in AS ISO-10993 [40]. These materials for extraction were also incubated for 24 h alongside with the tissue culture dishes. After 24 h, the media were removed and replaced with the extraction fluid followed by incubation for a further 48 h. Samples that were not exposed to extraction media (null) were replenished with fresh media instead. Following the incubation period (48 h), trypsin: osmol (1 mL, 50:50 vol %) was used to detach the cells from the dish. The cell number and viability were determined using a Vi-Cell XR Cell viability analyser based on trypan blue. Controls used include: EMEM media (null), extraction media, 4% ethanol, 5% ethanol, 7.5% ethanol.

CGI was expressed as a ratio of the number of cells in test material to the number of cells in PU control. A ratio of 0.7 or higher was considered an 'acceptable level' of cell growth inhibition within this assay [29,30]. Materials were performed in triplicates and the assay was repeated in triplicates.

3.8. In vitro *Heparin Release*

Heparin released from the coils was measured using the method described by Jaques *et al.* [41]. The method was based on the measurement of the metachromatic activity of heparin with Azure A. Coils were cut into 4 smaller sections and released in phosphate buffered saline (PBS, 10 mL) at 37 °C. Aliquots (400 μL) were taken at regular intervals and the sink replenished for a total of 24 h. Azure A was first dissolved in PBS at 0.1 mg/mL and this solution (60 μL) was added to the sample (150 μL). The solution was then mixed and absorbance measured by a spectrofluorometer at 492 nm (SpectraMax M2, Molecular Devices, CA, USA). Standards were prepared by a dilution series of heparin and PBS. PU coils without heparin was used as a control. The assay was repeated three times, where two of the assays were released for a further 24 h (total of 48 h) to determine the point at which the drug release profile plateaus.

Statistical analysis was performed using a two-way analysis of variance (ANOVA) to assess the effects of release time (24 *versus* 48 h). Individual comparisons between PU and the NCs were made with Dunnett's test. Significant difference was indicated by $p < 0.05$.

3.9. Thrombin Generation Assay

Blood was collected through venipuncture from donors that had not taken aspirin or any anticoagulants for at least 2 weeks prior to the experiment. Blood (9 part) was collected in a plastic tube containing 0.13 M sodium citrate (1 part). Platelet rich plasma (PRP) was isolated by centrifuging whole blood at 200 *g* for 15 min.
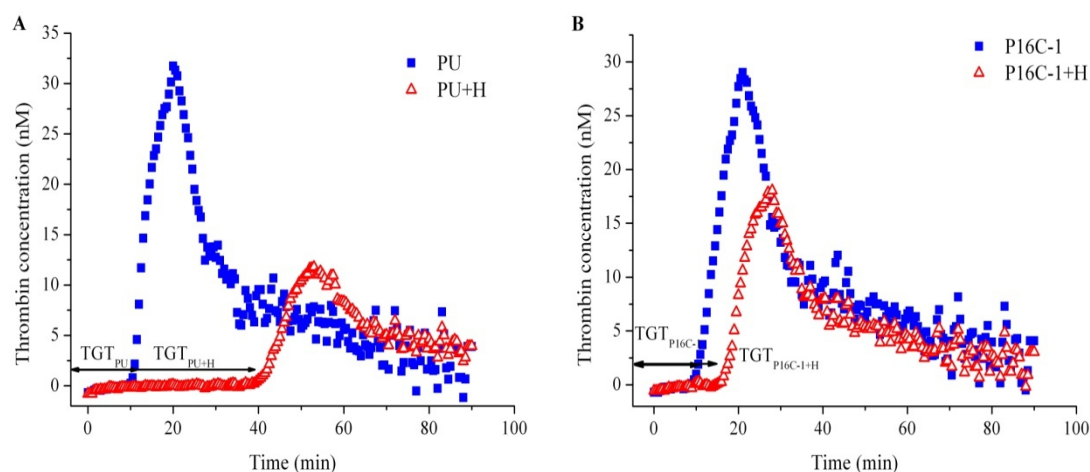
Each thrombin generation assay was performed with PRP from a single donor to ensure consistency. A pilot study was first conducted on samples that have been washed for different periods of time. Samples were washed prior to the start of the experiment for 24, 48 h and 7 days. The aim of this experiment was to examine if the surface heparin was still active after extensive washing and to determine the time required to remove to all residue heparin that could have affected the clotting time. Samples tested were PU + H and P16C-1 + H.

After determining the time required to remove all residue heparin from the pilot study described previously, thrombin generation assay was conducted on the coated coils. Two donors on different days were tested. Each assay consisted of 4 independent samples and the assay was repeated at least three times. The coils were first washed with PBS for at least 24 h (as determined from the pilot study) to remove all loosely attached heparin. A fluorogenic substrate for thrombin, Z-Gly-Gly-Arg-AMC (Bachem Holding, Bubendorf, Switzerland) was added to PRP to achieve a final concentration of 400 μM. The PRP was then recalcified by adding $CaCl_2$ (0.5 M stock solution) to a final concentration of $CaCl_2$ (20 mM). Recalcified PRP (200 μL) containing the fluorogenic substrate was then quickly transferred into 96 well plates that contains the coils. Fluorescence was measured by a spectrofluorometer. A kinetic measurement was taken at $\lambda_{ex} = 368$ nm and $\lambda_{em} = 460$ nm for a total duration of 90 min at 30 s interval. Teflon and blank wells were used as a positive and negative control respectively.

The intensity of the readings was then converted into a thrombin concentration in nanomolarity as described by Hemker *et al.* [42]. The resulted thrombin generation curve, as shown in Figure 9 was used to determine the thrombin generation lag time (TGT) and peak thrombin. TGT is defined as the time at which thrombin rises steeply, marking the start of clotting. The threshold value in this experiment is taken at 2 nM and the estimated time between when the blood first contact the material to when it rises above 2 nM is the lag time (TGT). Therefore, materials that are more thrombogenic have shorter TGTs compared to materials that are less thrombogenic.

Statistical analysis was performed using a two-way analysis of variance (ANOVA) to assess the effects of washing time on TGT. Individual comparisons between PU and NCs were made with Dunnett's test. A second two-way analysis (ANOVA) was performed to assess the difference between coils with and without heparin. Significant difference was indicated by $p < 0.05$.

Figure 9. Representative thrombin generation curves for: (**A**) PU and (**B**) P16C-1. Both experiments were simultaneously performed with PRP from a single donor. The time between the start of the experiment and the sudden rise in thrombin levels represents the thrombin generation lag time (TGT). Notice how the onset of thrombin between the controls and samples with heparin differs.

4. Conclusions

PUNCs were successfully coated onto stainless steel wires with no observable breakage or delamination when the wires were coiled. The dispersion of silicates was dependent on both the type of modifier and the silicate loading. Better dispersion was achieved with P16C-1 that showed a partially exfoliated structure, whereas samples with higher clay loadings and shorter alkyl chains showed an intercalated morphology and larger aggregates. The addition of silicate particles resulted in slightly lower CGI ratios as compared to pristine PU, but within the acceptable level of inhibition and the cells maintained a high viability. Blood compatibility of PUNCs as assessed by thrombin generation assays showed that the addition of silicate particles did not significantly decrease the thrombin generation lag time or the peak thrombin of PU. Although the addition of heparin in the nanocomposite system further improved the thrombin generation lag times, the large burst effect and low amounts of heparin released from coils suggested that the release was mainly from loosely attached heparin residues on the surface rather than via diffusion from the bulk polymer. This study demonstrated the feasibility of using PUNC systems as coatings for blood related applications. The size of the drug, interactions with the NC system, and biological activities are all important factors that need to be considered for PUNC as a controlled drug delivery system. Future studies will be conducted to assess whether this system can provide long term delivery or for dual drug release by selecting drugs that are smaller in molecular size and do not exhibit strong charge interactions with the NC system.

Acknowledgments

References

1. Hehrlein, C.; Arab, A.; Bode, C. Drug-eluting stent: The "magic bullet" for prevention of restenosis? *Basic Res. Cardiol.* **2002**, *97*, 417–423.

2. *Coronary Stenting: A Literature Review*; Australian Health Technology Advisory Committee: Canberra, Australia, 1997.

3. Knetsch, M.L.W. Blood-contacting surfaces. In *Biomaterials Fabrication and Processing*; Chu, P.K., Liu, X., Eds.; CRC Press: Boca Raton, Florida, 2008.

4. Ikada, Y. Surface modification of polymers for medical applications. *Biomaterials* **1994**, *15*, 725–736.

5. Han, D.K.; Park, K.D.; Ahn, K.D.; Jeong, S.Y.; Kim, Y.H. Preparation and surface characterization of PEO-grafted and heparin immobilized polyurethanes. *J. Biomed. Mater. Res.* **1989**, *23*, 87–104.

6. Du, Y.J.; Klement, P.; Berry, L.R.; Tressel, P.; Chan, A.K.C. *In vivo* rabbit acute model tests of polyurethane catheters coated with a novel antithrombin-heparin covalent complex. *Thromb. Haemost.* **2005**, *94*, 366–372.

7. Zhou, Z.; Meyerhoff, M.E. Preparation and characterization of polymeric coatings with combined nitric oxide release and immobilized active heparin. *Biomaterials* **2005**, *26*, 6506–6517.

8. Riedl, C.R.; Witkowski, M.; Plas, E.; Pflueger, H. Heparin coating reduces encrustation of ureteral stents: A preliminary report. *Int. J. Antimicrobial Agents* **2002**, *19*, 507–510.

9. Fu, J.; Ji, J.; Fan, D.; Shen, J. Construction of antibacterial multilayer films containing nanosilver via layer-by-layer assembly of heparin and chitosan-silver ions complex. *J. Biomater. Res.* **2006**, *79*, 665–674.

10. Tan, Q.; Ji, J.; Barbosa, M.A.; Fonseca, C.; Shen, J. Constructing thromboresistant surface on biomedical stainless steel via layer-by-layer deposition anticoagulant. *Biomaterials* **2003**, *24*, 4699–4705.

11. Tan, Q.; Ji, J.; Zhao, F.; Fan, D.Z.; Sun, F.Y.; Shen, J.C. Fabrication of thromboresistant multilayer thin film on plasma treated poly(vinyl chloride) surface. *J. Mater. Sci-Mater. Med.* **2005**, *16*, 687–692.

12. Van der Heiden, A.P.; Goebbels, D.; Pijpers, A.P.; Koole, L.H. A photochemical method for the surface modification of poly(etherurethanes) with phosphorylcholine-containing compounds to improve hemocompatibility. *J. Biomater. Res.* **1997**, *37*, 282–290.

13. Desai, N.P.; Hubbell, J.A. Solution technique to incorporate polyethylene oxide and other water-soluble polymers into surfaces of polymeric biomaterials. *Biomaterials* **1991**, *12*, 144–153.

14. Mazid, M.A.; Scott, E.; Nai-Hong, L. New biocompatible polyurethane-type copolymer with low molecular weight heparin. *Clin. Mater.* **1991**, *8*, 71–80.

15. Labarre, D.; Jozefowicz, M.; Boffa, M.C. Properties of heparin-poly (methyl methacrylate) copolymers. II. *J. Biomed. Mater. Res.* **1977**, *11*, 283–295.

16. Moon, H.T.; Lee, L.K.; Han, J.K.; Byun, Y. A novel formulation for controlled release of heparin-DOCA conjugate dispersed as nanoparticles in polyurethane film. *Biomaterials* **2001**, *22*, 281–289.

17. Huang, X.; Brazel, C.S. On the importance and mechanisms of burst release in matrix-controlled drug delivery systems. *J. Control. Release* **2001**, *73*, 121–136.

18. Deconinck, E.; Sohier, J.; Scheerder, I.D.; Van den Mooter, G. Pharmaceutical aspects of drug eluting stents. *J. Pharm. Sci.* **2008**, *97*, 5047–5060.

19. Chen, M.C.; Chang, Y.; Liu, C.T.; Lai, W.Y.; Peng, S.F.; Hung, Y.W.; Tsai, H.W.; Sung, H.W. The characteristics and *in vivo* suppression of neointimal formation with sirolimus-eluting polymeric stents. *Biomaterials* **2009**, *30*, 79–88.

20. Lee, P.I. Effect of non-uniform initial drug concentration distribution on the kinetics of drug release from glassy hydrogel matrices. *Polymer* **1984**, *25*, 973–978.

21. Endo, M.; Koyama, S.; Matsuda, Y.; Hayashi, T.; Kim, Y.A. Thrombogenicity and blood coagulation of a microcatheter prepared from carbon nanotubes-nylon based composite. *Nano lett.* **2004**, *5*, 101–105.

22. Kannan, R.Y.; Salacinski, H.J.; Groot, J.D.; Clatworthy, I.; Bozec, L.; Horton, M.; Butler, P.E.; Seifalian, A.M. The antithrombogenic potential of a polyhedral oligomeric silsesquioxane (POSS) nanocomposite. *Biomacromolecules* **2006**, *7*, 215–223.

23. Zhou, N.; Fang, S.; Xu, D.; Zhang, J.; Mo, H.; Shen, J. Montmorillonite-phosphatidyl choline/PDMS films: A novel antithrombogenic material. *Appl. Clay Sci.* **2009**, *46*, 401–403.

24. Koh, L.B.; Rodriguez, I.; Zhou, J. Platelet adhesion studies on nanostructured poly(lactic-co-glycolic-acid)-carbon nanotube composite. *J. Biomater. Res.* **2008**, *86*, 394–401.

25. Asmatulu, R.; Claus, R.O.; Mecham, J.B.; Corcoran, S.G.; Wang, Y.X. Nanocomposite thin film coatings for protection of materials surfaces. *MRS Proc.* **2005**, *872*, J13.14.1–J13.14.6.

26. Zaporojtchenko, V.; Podschun, R.; Schürmann, U.; Kulkarni, A.; Faupel, F. Physico-chemical and antimicrobial properties of co-sputtered Ag–Au/PTFE nanocomposite coatings. *Nanotechnol.* **2006**, *17*, 4904.

27. Lamba, N.M.K.; Woodhouse, K.A.; Cooper, S.L. *Polyurethanes in Biomedical Applications*; Schapiro, F., Ed.; CRC Press: Boca Raton, FL, USA, 1997.

28. Poole-Warren, L.A.; Farrugia, B.; Fong, N.; Hume, E.; Simmons, A. Controlling cell-material interactions with polymer nanocomposites by use of surface modifying additives. *Appl. Surf. Sci.* **2008**, *255*, 519–522.

29. Zhu, H.; Kumar, A.; Ozkan, J.; Bandara, R.; Ding, A.; Perera, I.; Steinberg, P.; Kumar, M.; Lao, W.; Griesser, S.S.; *et al.* Fimbrolide-coated antimicrobial lenses: Their *in vitro* and *in vivo* effects. *Optometry Vision Sci.* **2008**, *85*, 292–300.

30. Baveja, J.K.; Willcox, M.D.P.; Hume, E.B.H.; Kumar, N.; Odell, R.; Poole-Warren, L.A. Furanones as potential anti-bacterial coatings on biomaterials. *Biomaterials* **2004**, *25*, 5003–5012.

31. Styan, K.E.; Martin, D.J.; Poole-Warren, L.A. *In vitro* fibroblast response to polyurethane organosilicate nanocomposites. *J. Biomed. Mater. Res. Part A* **2008**, *86*, 571–582.

32. Joshi, G.V.; Patel, H.; Bajaj, H.; Jasra, R. Intercalation and controlled release of vitamin B_6 from montmorillonite-vitamin B_6 hybrid. *Colloid Polym. Sci.* **2009**, *287*, 1071–1076.

33. Suggs, L.J.; Shive, M.S.; Garcia, C.A.; Anderson, J.M.; Mikos, A.G. *In vitro* cytotoxicity and *in vivo* biocompatibility of poly(propylene fumarate-co-ethylene glycol) hydrogels. *J. Biomed. Mater. Res.* **1999**, *46*, 22–32.

34. Rosengren, A.; Faxius, L.; Tanaka, N.; Watanabe, M.; Bjursten, L.M. Comparison of implantation and cytotoxicity testing for initially toxic biomaterials. *J. Biomed. Mater. Res. Part A* **2005**, *75*, 115–122.

35. Bounameaux, H. Unfractionated *versus* low-molecular-weight heparin in the treatment of benous thromboembolism. *Vasc. Med.* **1998**, *3*, 41.

36. Munro, M.S.; Eberhart, R.C.; Maki, N.J.; Brink, B.E.; Fry, W.J. Thromboresistant alkyl derivatized polyurethanes. *ASAIO*. **1983**, *6*, 65–75.

37. Duncan, A.C.; Sefton, M.V.; Brash, J.L. Effect of C_4-, C_8- and C_{18}- alkylation of poly(vinyl alcohol) hydrogels on the adsorption of albumin and fibrinogen from buffer and plasma: Limited correlation with platelet interactions. *Biomaterials* **1997**, *18*, 1585–1592.

38. Courtney, J.M.; Lamba, N.M.K.; Sundaram, S.; Forbes C.D. Biomaterials for blood-contacting applications. *Biomaterials* **1994**, *15*, 737–744.

39. Heuck, C.C.; Schiele, U.; Horn, D.; Fronda, D.; Ritz, E. The role of surface charge on the accelerating action of heparin on the antithrombin III-inhibited activity of α-Thrombin. *J. Biol. Chem.* **1985**, *260*, 4598–4603.

40. *Biological Evaluation of Medical Devices*; AS-ISO-10993; Standards Australia International Ltd: Sydney, Austrilia, 2004.

41. Jaques, L.B.; Monkhouse, F.C.; Stewart, M. A method for the determination of heparin in blood. *J. Physiol.* **1949**, *109*, 41–48.

42. Hemker, H.C.; Giesen, P.; AlDieri, R.; Regnault, T.; de Smed, E.; Wagenvoord, R. The calibrated automated thrombogram (CAT): A universal routine test for hyper- and hypocoagulability *Pathophysiol. Haemost. Thromb.* **2002**, *32*, 249–253.